

CheXNet: Combing Transformer and CNN for Thorax Disease Diagnosis from Chest X-ray Images (Supplementary material)

Xin Wu¹, Yue Feng^{1(✉)}, Hong Xu^{1,2}, Zhuosheng Lin¹, Shengke Li¹, Shihan Qiu¹, QiChao Liu¹, and Yuangang Ma¹

¹ Faculty of Intelligent Manufacturing, Wuyi University, Jiangmen 529020, Guangdong, China

² Institute for Sustainable Industries and Liveable Cities, Victoria University, Melbourne 8001, Australia

✉Corresponding author: J002443@wuyi.edu.cn

In this supplement, we describe the CXR11 and CXR14 datasets in further detail. The classification performance of the proposed CheXNet in CXR11 and CXR14 is then qualitatively compared with other eight networks.

A Dataset

We used data from the CXR11 and CXR14 public dataset sections, as described in the footnote¹.

CXR11 Each image may have one or more types of catheter placement. Fig. 1 shows the number of CXR11 images for each disease.

CXR14 The NIH ChestX-ray14 dataset, which is an extension of the ChestX-ray8 [1], includes 112120 frontal X-ray images from 30805 unique patients with annotations for 14 common diseases. The images have a size of 1024×1024 pixels and are from special patient populations. Due to computational limitations, this study performed multi-label sample classification on 51759 CXR images, named CXR14, rather than the complete set of 112120 frontal images. Table 1 shows the number of CXR14 images for each disease.

A.1 Comparison to the State-of-the-Arts

For comparison with other algorithms and to demonstrate the overall performance of the network, Fig. 2 a) illustrates the ROC curves on the CXR11 dataset, where the curves are more effective the closer they are to the upper left. The radar plot in Fig. 2 b) illustrates the AUC values for each disease on the CXR11 dataset, where the red curve representing our method is closer to the outermost arc, further confirming its effectiveness. Similarly for the data set CXR14, Fig. 3 a) illustrates the ROC curves on the CXR11 data set and Fig. 3 b) the radar plot illustrates the AUC values for the 14 diseases on the CXR14 data set.

¹ <https://github.com/wuliwuxin/CheXNet>

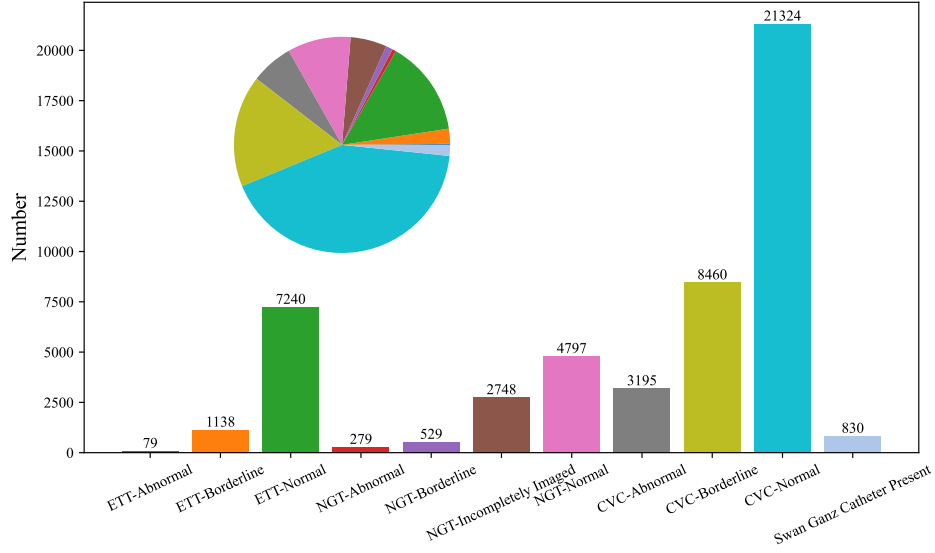


Fig. 1. Comparison of the number of cases for each disease in the CXR11 dataset.

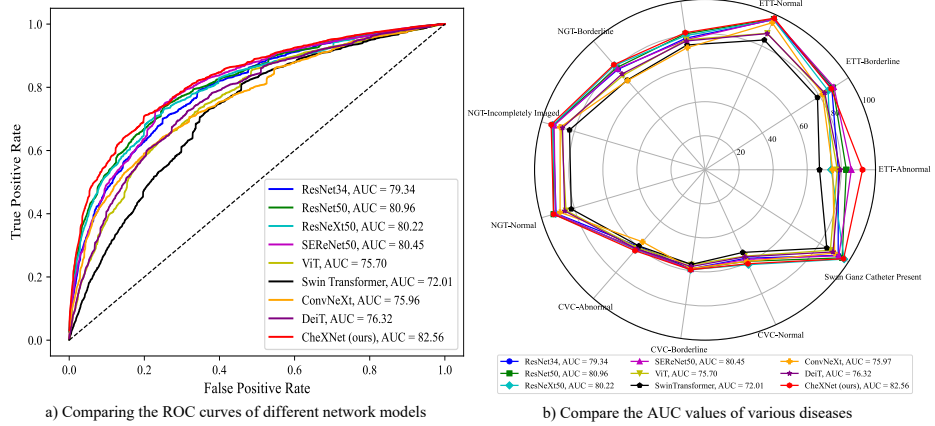


Fig. 2. Comparison of the average AUC scores (%) of CheXNet and 8 common networks on the CXR11 dataset. a) Compare the ROC curves of different network models; b) Compare the diagnostic model performance of 11 diseases.

Table 1. The number of CXR14 images each disease. There are serious data imbalances, for example, there are many more Infiltration images than Hernia images.

Disease	Number	Percentage	Disease	Number	Percentage
Atelectasis	11559	22.32%	Hernia	156	0.31%
Cardiomegaly	2406	4.65%	Infiltration	11794	22.77%
Consolidation	3330	6.44%	Mass	2927	5.66%
Edema	1862	3.60%	Nodule	3002	5.80%
Effusion	8038	15.52%	Pleural Thickening	1216	2.35%
Emphysema	1733	3.35%	Pneumonia	327	0.64%
Fibrosis	1215	2.35%	Pneumothorax	2194	4.24%

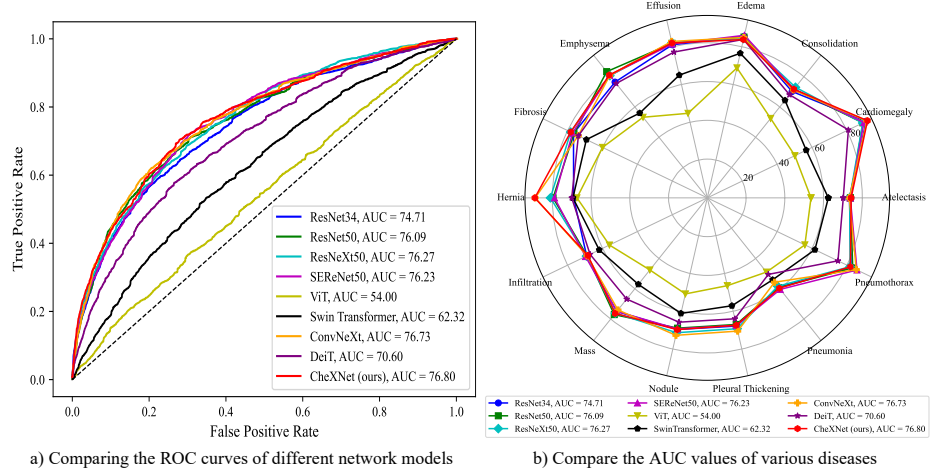


Fig. 3. Comparison of the average AUC scores (%) of CTransCNN and 8 common networks on CXR dataset. a) Compare the ROC curves of different network models; b) Compare the diagnostic model performance of 14 diseases.

References

1. Wang, X., Peng, Y., Lu, L., Lu, Z., Bagheri, M., Summers, R.M.: Chestx-ray8: Hospital-scale chest x-ray database and benchmarks on weakly-supervised classification and localization of common thorax diseases. In: Proceedings of the IEEE Conference on Computer Vision and Pattern Recognition (CVPR) (July 2017), Honolulu, HI (2017)